



A Photocatalyst Based in Pelargonidin 3-Glucoside as Dye Sensitizer on Small TiO₂ Nanoclusters

M.A. Flores-Hidalgo^{1**}, D. Barraza-Jiménez¹, L.F. Lozano-Silva¹, M.A. Escobedo-Bretado¹, V. Collins- Martinez², A. López Ortiz², A. Martínez de la Cruz³

¹Universidad Juárez del Estado de Durango, Facultad de Ciencias Químicas, Av. Veterinaria S/N, Circuito Universitario, Durango, Dgo. México, C.P. 34120. *Tel: +526181881941

email: maflores.hidalgo@gmail.com

²Centro de Investigación en Materiales Avanzados, S.C., Departamento de Ingeniería y Química de Materiales, Miguel de Cervantes 120, Chihuahua, Chih., México, 31109

³Facultad de Ingeniería Mecánica y Eléctrica, Universidad Autónoma de Nuevo León, Ciudad Universitaria, C.P. 66451, San Nicolás de los Garza, N.L., México

Four small TiO₂ nanoclusters sensitized with pelargonidin 3-glucoside (C₂₁H₂₁O₁₀⁺), a natural pigment derived from anthocyanidin. A model of the sensitization interaction between the nanoclusters and the natural pigment was developed and its geometric features as well as its electronic structure properties are studied. DFT methods were used to obtain geometries and a frequencies analysis was carried out to assure global minima. Ground states were calculated for the individual nanostructures and pelargonidin. Next the interaction between a nanocluster with the pigment was studied and its geometric parameters for better results are proposed. Energies were obtained for the individual nanoclusters and pigment at their ground state and the same methodology was applied to the interacting systems. HOMO, LUMO, band gap, chemical properties and other features are discussed. The sensitization process output is several interesting dye sensitized nanoclusters for photocatalysis applications with strong attraction to negative charge and a reduction on their band gap.

Keywords—TiO₂ nanoclusters; sensitized; photocatalysis; DFT.

I. INTRODUCTION

It is an undergoing task the search for cleaner methods to produce hydrogen. For this process, the use of alternative energy such as solar, eolic, geothermic, among others etc. as precursor to obtain hydrogen is a good possibility as cleaner technology [1]. Within these alternative energy options our work focuses in solar energy using photocatalysis. In photocatalysis the photocatalyzer plays a major role and the its critical success factors depend on properties such as chemical stability, creep resistance, visible light absorption, appropriate energy bands, etc.[2] It is well known the more used photocatalyzer is titanium dioxide (TiO₂) due to its better features for this application and there is a lot of work in this matter either trying to improve its properties or finding alternative semiconducting metal oxides that may perform similarly [3-4]. Due to its outstanding performance the use of TiO₂ as photocatalyzer has extended to water dissociation, pollutants degradation, organic selective transformations, CO₂ sequestration for fuel generation, etc. [5-6] There are several techniques to improve TiO₂ properties, in

this work we will use nanostructured TiO₂ in its cluster presentation and a sensitization of the semiconducting oxide using a natural pigment. A model of the sensitized nanostructure was built and density functional theory is used to carry out electronic structure calculations. The sensitized material properties are discussed. Properties such us band gap, HOMO, LUMO, IP, EA, among others are displayed within this work and insights on the potential on this material for photocatalysis applications.

II. THEORY AND COMPUTATIONAL DETAILS

Theoretical calculations were performed in Gaussian09 programs suite [7]. (TiO₂)_n nanostructures, pelargonidin and nanostructured systems containing both molecules were relaxed. Pelargonidin is used as a (+1) cation and was treated with B3LYP/6-311+g(d,p). (TiO₂)_n nanostructures were built resembling previously reported geometric parameters [8-10]. Energy calculations were performed for all molecules to find the electronic properties such as HOMO, LUMO, gap, ionization potential (IP), electronic affinity (EA), electrophilicity (ω), electronegativity (χ), hardness (η), and Fukui functions with the same theoretical method.

Geometry optimizations and vibrational frequency analyses were carried out using DFT with the well-known B3LYP approach, which includes the interchange hybrid functional from Becke [11] in combination with the correlation functional three parameter by Lee-Yang-Parr [12], and 6-311g(d) basis set as implemented in Gaussian09 program package. Based on literature and our method validation results, we propose B3LYP/6-311+g(d,p) theoretical method provides good results with a good level of accuracy for these systems and will be used to carry on with the rest of the work. We considered some variants of (TiO₂)_n nanoclusters already studied theoretically and used the same geometric parameters to build the input structures. The work was done this way under the assumption that the structure feasibility was already proved by Hamad et al. and other research teams [8-10]. In their works when these (TiO₂)_n were proposed. Then we made the geometry optimization of (TiO₂)_n nanoclusters and applied the

sensitization by bonding a single pelargonidin molecule at each nanocluster to create new structures. Our theoretical calculations used a different theoretical method since we used DFT in contrast to the genetic algorithm used on the referred works. We present a single variant for each size of the $(\text{TiO}_2)_n$ nanoclusters as shown in Fig. 1, all of them optimized at the same theoretical level in its pure form. Then we used the optimized nanocluster to add the pelargonidin molecule as sensitizer material and relaxed the new geometry with the same theoretical method. Each geometry optimization was followed by a calculation of harmonic vibrational frequencies to confirm that the optimized geometry corresponds to a local minimum. The zero-point vibrational energy (ZPVE) scaling and the thermal correction (TC) at 298.15 K were also performed. Our results are compared with the literature to verify the geometric parameters for the nanostructures in their pristine form. We also used as reference the generally accepted TiO_2 in its bulk presentation as basis to compare how much the bond length and angles in our study differ from a commonly known bond or angle within TiO_2 simple crystals.

III. RESULTS AND DISCUSSION

Four nanocluster geometries were modeled according to recommended parameters within the literature. This nanostructures were relaxed and treated for energy computations with B3LYP/6-311+g(d,p). With this theoretical method it was achieved good accuracy in comparison with computational time. Nanocluster geometries showed bond length values near 1.8 Å for Ti-O. Dihedral angles values were near to the reported $113^\circ \pm 5^\circ$ [13]. Pigment geometry behaved similarly to nanoclusters with bond length and angles in agreement with known values for these organic molecules. Pristine TiO_2 nanoclusters and pelargonidin geometry calculations agreed with literature reported parameters in general, without any relevant additional insight.

Pristine nanoclusters and pigment and its ground states were used to build a model to represent interactions between them. Variants of the nanosystems formed by the nanocluster and the natural dye are displayed in Fig. 2.

During the exercise of finding the best location for nanostructures interaction with the organic molecules we calculated the Fukui functions (Tables 5 and 6). However, our best approach during the search process for best location was based on attempting to locate the nanocluster more accessible Ti atom with the outer pigment oxygens. For pelargonidin the dangling oxygens are good places for interactions with the selected semiconductor oxide.

Different external oxygens around the pigment allowed us to locate the interaction atoms in different places. The more accessible Ti atom was selected to interact with the pigment oxygens. It was observed weak interactions were possible between pigment molecule and nanostructures for the sensitized nanosystems with a Ti-O bond size near 2.0 Å. We tested interactions with other bond lengths, distances were increased in 0.1 Å increments over the 2.0 Å with unsuccessful results because resulting structures were unstable.

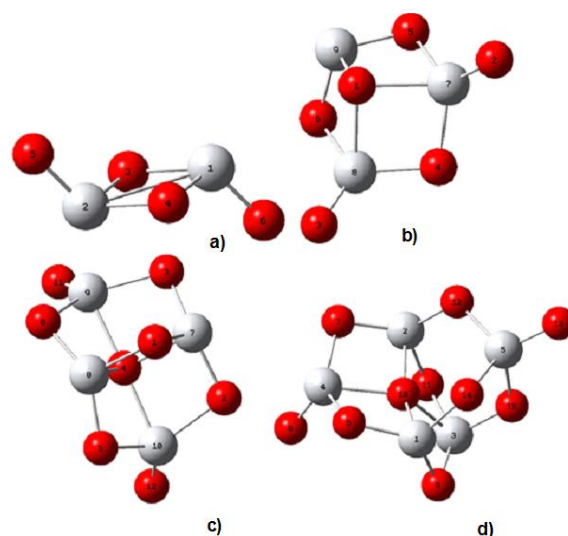


Fig. 1. Nanostructures sensitized. In light grey Ti atoms in red oxygen atom

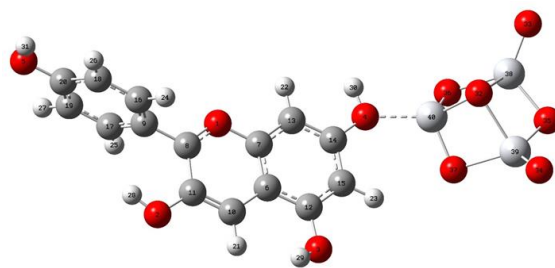


Fig. 2. Interaction model of $(\text{TiO}_2)_3$ (right side) nanocluster with pelargonidin (left side).

Table 1. Energy calculations. E_{min} is minimum energy and E_{g} is HOMO-LUMO gap. All units in eV.

| Nanocluster | E_{min} | E_{g} | HOMO | LUMO |
|--|------------------|----------------|---------|--------|
| $(\text{TiO}_2)_2$ | -25961.62 | 2.881 | -10.080 | -7.200 |
| $(\text{TiO}_2)_3$ | -54423.40 | 5.021 | -8.076 | -3.054 |
| $(\text{TiO}_2)_4$ | -81637.60 | 3.753 | -7.952 | -4.199 |
| $(\text{TiO}_2)_5$ | -108852.00 | 5.159 | -8.717 | -3.558 |
| $(\text{C}_{15}\text{H}_{11}\text{O}_5)^+$ | -136066.20 | 4.889 | -8.608 | -3.719 |

Table 2. Chemical properties obtained with conceptual DFT. All units in eV.

| Cluster/Molec | PI | EA | χ | η | μ | ω | S |
|--|--------|-------|--------|--------|--------|----------|-------|
| $(\text{TiO}_2)_2$ | 10.416 | 1.516 | 5.966 | 4.450 | 0.225 | 0.670 | 0.225 |
| $(\text{TiO}_2)_3$ | 9.915 | 2.588 | 6.251 | 3.664 | 0.273 | 0.853 | 0.273 |
| $(\text{TiO}_2)_4$ | 10.501 | 1.786 | 6.143 | 4.357 | 0.229 | 0.705 | 0.230 |
| $(\text{TiO}_2)_5$ | 10.221 | 2.215 | 6.218 | 4.003 | 0.250 | 0.777 | 0.250 |
| $(\text{C}_{15}\text{H}_{11}\text{O}_5)^+$ | 11.653 | 5.701 | 8.677 | 2.976 | -8.677 | 12.649 | 0.336 |



Table 3. Energy calculations for interacting nanoclusters and pelargonidin. $a=(\text{TiO}_2)_2$, $b=(\text{TiO}_2)_3$, $c=(\text{TiO}_2)_4$, $d=(\text{TiO}_2)_5$. All units in eV.

| Variant | E _{min} | E _g | HOMO | LUMO |
|------------------------|------------------|----------------|---------|--------|
| Variant ^a 1 | -80389.625 | 2.749 | -9.794 | -7.045 |
| Variant ^a 2 | -80393.835 | 2.967 | -9.694 | -6.728 |
| Variant ^a 3 | -80390.120 | 3.027 | -9.861 | -6.833 |
| Variant ^a 4 | -80389.430 | 2.401 | -9.592 | -7.191 |
| Variant ^b 1 | -107605.452 | 2.910 | -9.805 | -6.896 |
| Variant ^b 2 | -107605.740 | 2.778 | -9.496 | -6.718 |
| Variant ^b 3 | -107605.392 | 3.026 | -9.990 | -6.964 |
| Variant ^b 4 | -107605.056 | 2.912 | -9.881 | -6.968 |
| Variant ^c 1 | -134820.511 | 2.898 | -9.948 | -7.050 |
| Variant ^c 2 | -134820.588 | 2.932 | -9.867 | -6.935 |
| Variant ^c 3 | -134820.645 | 3.015 | -10.025 | -7.010 |
| Variant ^c 4 | -134820.545 | 2.918 | -10.115 | -7.197 |
| Variant ^d 1 | -162036.180 | 2.620 | -9.914 | -7.294 |
| Variant ^d 2 | -162036.458 | 2.864 | -9.699 | -6.835 |
| Variant ^d 3 | -162036.165 | 3.071 | -9.804 | -6.733 |
| Variant ^d 4 | -162036.244 | 3.035 | -10.086 | -7.051 |

Table 4. Chemical properties obtained with conceptual DFT corresponding to interacting nanoclusters and pelargonidin. All units in eV.

| Cluster/Molec | PI | EA | χ | η | μ | ω | S |
|------------------------|--------|-------|--------|--------|--------|----------|-------|
| Variant ^a 1 | 11.073 | 5.628 | 8.351 | 2.723 | -8.351 | 12.806 | 0.367 |
| Variant ^a 2 | 11.115 | 6.191 | 8.653 | 2.462 | -8.653 | 15.206 | 0.406 |
| Variant ^a 3 | 11.226 | 5.437 | 8.332 | 2.895 | -8.332 | 11.991 | 0.346 |
| Variant ^a 4 | 11.087 | 5.736 | 8.412 | 2.675 | -8.412 | 13.224 | 0.374 |
| Variant ^b 1 | 11.072 | 5.513 | 8.293 | 2.778 | -8.293 | 12.369 | 0.360 |
| Variant ^b 2 | 10.846 | 5.381 | 8.113 | 2.732 | -8.113 | 12.046 | 0.366 |
| Variant ^b 3 | 11.299 | 5.603 | 8.451 | 2.848 | -8.451 | 12.537 | 0.351 |
| Variant ^b 4 | 11.211 | 5.502 | 8.356 | 2.855 | -8.356 | 12.231 | 0.350 |
| Variant ^c 1 | 11.208 | 5.666 | 8.437 | 2.771 | -8.437 | 12.844 | 0.361 |
| Variant ^c 2 | 11.153 | 5.569 | 8.361 | 2.792 | -8.361 | 12.518 | 0.358 |
| Variant ^c 3 | 11.326 | 5.654 | 8.490 | 2.836 | -8.490 | 12.709 | 0.353 |
| Variant ^c 4 | 11.243 | 5.760 | 8.506 | 2.742 | -8.502 | 13.182 | 0.365 |
| Variant ^d 1 | 11.097 | 5.893 | 8.495 | 2.602 | -8.495 | 13.865 | 0.384 |
| Variant ^d 2 | 11.030 | 5.498 | 8.264 | 2.766 | -8.264 | 12.346 | 0.362 |
| Variant ^d 3 | 11.097 | 5.893 | 8.495 | 2.602 | -8.495 | 13.865 | 0.384 |
| Variant ^d 4 | 11.271 | 5.630 | 8.450 | 2.820 | -8.450 | 12.660 | 0.355 |

Energy calculations were carried out to understand the newly formed sensitized nanostructures using B3LYP/6-311+g(d,p). We calculated the minimum energy for pristine TiO_2 nanoclusters at its ground states and then applied a similar theoretical method for dye sensitized nanoclusters.

Table 5. Fukui functions for nanoclusters. Units in eV.

| Nanocluster | fk^+ | fk^- | fk^0 |
|--------------------|----------------|----------------|----------------|
| $(\text{TiO}_2)_2$ | 0.389 O3, O4 | 0.202 O5, O6 | 0.284 Ti1, Ti2 |
| $(\text{TiO}_2)_3$ | 0.556 Ti9 | 0.185 O2, O3 | 0.327 Ti9 |
| $(\text{TiO}_2)_4$ | 0.199 Ti7, Ti8 | 0.121 O11, O12 | 0.141 Ti7, Ti8 |
| $(\text{TiO}_2)_5$ | 0.325 Ti2 | 0.161 O13 | 0.191 Ti2 |

Table 6. Fukui functions for pelargonidin. Units in eV.

| Pelargonidin | fk^+ | fk^- | fk^0 |
|--|-----------|-----------|-----------|
| $(\text{C}_{15}\text{H}_{11}\text{O}_5)^+$ | 0.100 C13 | 0.140 C9 | 0.074 C13 |
| | 0.068 C14 | 0.131 C6 | 0.058 C9 |
| | 0.063 C13 | 0.104 C20 | 0.053 C20 |
| | 0.059 C7 | 0.076 O2 | 0.053 O2 |
| | 0.058 C19 | 0.061 O5 | 0.046 C6 |

Dye sensitization has a favorable effect in nanoclusters minimum energy without exception by decreasing its values. Minimum energy, HOMO-LUMO gap, HOMO and LUMO are shown in Tables 1 and 2.

Band gap for pristine nanoclusters are wide with $(\text{TiO}_2)_2$ and $(\text{TiO}_2)_4$ having the narrower values with 2.881 and 3.753 eV. Pigment has a wide band gap as well with a resulting value for pelargonidin of 4.889 eV. In order to obtain a reduction in TiO_2 band gap energy levels of nanocluster and pigment to mix and complement each other. With the proposed model all nanocluster variants reduce their band gap but depend largely in the nanocluster interaction location. The narrower band gap calculated with our DFT results was found in $(\text{TiO}_2)_2$ nanocluster variant with 2.401 eV. With the proposed model all nanocluster variants reduce their band gap but depend largely in the nanocluster interaction location. The narrower band gap found was found in $(\text{TiO}_2)_2$ with 2.401 eV. Pigment molecular orbitals have an effect on HOMO but the effect in LUMO is stronger and this contribution is the more significant to determine the gap. This is true for three nanocluster variants but $(\text{TiO}_2)_2$ is an exception. In $(\text{TiO}_2)_2$ pigment effect on its electronic structure is less and changes in HOMO and LUMO are smaller than in the other nanostructures.

Conceptual DFT was used to calculate chemical properties. These calculations indicate an increase in ionization potential, electron affinity and electronegativity of nanoclusters when dye sensitization was carried out. This effect may be due to the cation feature contributed by pelargonidin to the system. This positive charge provided by the pigment has also a noticeable effect in hardness and softness and it is even more evident in the electrophilicity index which shows a clear trend of the sensitized materials to attract electrons. Tables 3 and 4 display conceptual DFT.

Our research within these proceedings indicate sensitization of TiO_2 nanoclusters increase the potential of the nanoclusters for photocatalysis applications. Further calculations will be performed in the short term to continue analyzing electronic structure and charge transfer.

IV. CONCLUSIONS

Four nanocluster geometries were sensitized with pelargonidin. This work provides data to make the sensitization process more efficient from geometric parameters to electronic structure data. Sensitization process may work well with this nanoclusters and pelargonidin but the cation character of the pigment is present in the final systems. If attraction to electron charge is needed, then these nanomaterials may be a good



option. Further research to calculate charge transfer and more electronic structure data will aid to learn more about this photocatalyzer.

ACKNOWLEDGMENT

MAFH, DBJ and MAEB are researchers at FCQ-UJED and CONACYT. ALO and VHCM are researchers at CIMAV-CONACYT. AdelaCM is a researcher at FIME-UANL and CONACYT. This work was financed by SEP-CONACYT with DSA/103.5/15/7028 project supported by 2015 National PRODEP funding. Thanks to Dr. D. Glossman-Mitnik for his technical contribution.

REFERENCES

- [1] U.S. Department of Energy Hydrogen, Fuel Cells and Infrastructure Technologies Program, Hydrogen Posture Plan, U.S. Department of Energy, 2006. U.S.
- [2] J. Zhu, M. Zach, "Nanostructured materials for photocatalytic hydrogen production", current opinion in colloid interface science, [2009].
- [3] Chen X B, Mao S S. Chem Rev, 2007, 107: 2891.
- [4] Fujishima A, Honda K. Nature, 1972, 238: 37.
- [5] Wen, J.; Li, X.; Liu, W.; Fang, Y.; Xie, J.; Xu, Y. Photocatalysis fundamentals and surface modification of TiO₂ nanomaterials. Chinese Journal of Catalysis 2015, 36, 2049-2070.
- [6] Jenny Schneider, Masaya Matsuoka, Masato Takeuchi, Jinlong Zhang, Yu Horiuchi, Masakazu Anpo, and Detlef W. Bahnemann. Understanding TiO₂ Photocatalysis: Mechanisms and Materials. Chem. Rev. 2014, 114, 9919–9986.
- [7] Gaussian 09, Revision D.01, M. J. Frisch, G. W. Trucks, H. B. Schlegel, G. E. Scuseria, M. A. Robb, J. R. Cheeseman, G. Scalmani, V. Barone, B. Mennucci, G. A. Petersson, H. Nakatsuji, M. Caricato, X. Li, H. P. Hratchian, A. F. Izmaylov, J. Bloino, G. Zheng, J. L. Sonnenberg, M. Hada, M. Ehara, K. Toyota, R. Fukuda, J. Hasegawa, M. Ishida, T. Nakajima, Y. Honda, O. Kitao, H. Nakai, T. Vreven, J. A. Montgomery, Jr., J. E. Peralta, F. Ogliaro, M. Bearpark, J. J. Heyd, E. Brothers, K. N. Kudin, V. N. Staroverov, T. Keith, R. Kobayashi, J. Normand, K. Raghavachari, A. Rendell, J. C. Burant, S. S. Iyengar, J. Tomasi, M. Cossi, N. Rega, J. M. Millam, M. Klene, J. E. Knox, J. B. Cross, V. Bakken, C. Adamo, J. Jaramillo, R. Gomperts, R. E. Stratmann, O. Yazyev, A. J. Austin, R. Cammi, C. Pomelli, J. W. Ochterski, R. L. Martin, K. Morokuma, V. G. Zakrzewski, G. A. Voth, P. Salvador, J. J. Dannenberg, S. Dapprich, A. D. Daniels, O. Farkas, J. B. Foresman, J. V. Ortiz, J. Cioslowski, and D. J. Fox, Gaussian, Inc., Wallingford CT, 2013.
- [8] Woodley S.M., Hamad S., Mejías J. A. and Catlow C.R.A. Properties of small TiO₂, ZrO₂ and HfO₂ nanoparticles. J. Mater. Chem., 2006, 16, 1927–1933.
- [9] Syzgantseva O.A., Gonzalez-Navarrete P., Calatayud M., Bromley S., and Minot C. Theoretical Investigation of the Hydrogenation of (TiO₂)_N Clusters (N = 1-10). J. Phys. Chem. C 2011, 115, 15890.
- [10] Hamad, S.; Catlow, C. R. A.; Woodley, S. M.; Lago, S.; Mejias, J. A. Structure and Stability of Small TiO₂ Nanoparticles. J. Phys. Chem. B 2005, 109, 15741.
- [11] A.D. Becke. J.Chem Phys. 104 (1993) 5648.
- [12] C. Lee, R. Yang, G. Parr. Phys. Rev B, 37 (1988) 785.
- [13] Gribb, A.A. and Banfield, J.F. "Particle size effects on transformation kinetics and phase stability in nanocrystalline TiO₂" American Mineralogy (82) 717-728..